

Synthesis and Crystal Structure of the Organically Templated Open Framework Magnesium Phosphate UiO-20 with DTF Topology

Kjell Ove Kongshaug, Helmer Fjellvåg,* and Karl Petter Lillerud

Department of Chemistry, University of Oslo, P.O. Box 1033 Blindern, N-0315 Oslo, Norway

Received November 16, 1999. Revised Manuscript Received January 14, 2000

The synthesis and crystal structure of $\text{Mg}_4(\text{PO}_4)_4 \cdot 2\text{C}_2\text{H}_{10}\text{N}_2$ (UiO-20), which is the first example of an organically templated open framework magnesium phosphate, is described. UiO-20 is characterized by means of single-crystal and powder X-ray diffraction, solid-state ^{31}P MAS NMR spectroscopy, and thermogravimetric analysis. Crystal data for UiO-20: space group $C2/c$ (no. 15); $a = 20.9098(8)$ Å, $b = 17.8855(7)$ Å, $c = 14.7913(6)$ Å; $\gamma = 134.842(2)^\circ$; $V = 3922.3(3)$ Å³; and $Z = 8$. The framework topology is of zeolite type DFT, and UiO-20 is isostructural with compounds such as the cobalt phosphate DAF-2, zinc phosphate DAF-3, zinc arsenate UCSB-3ZnAs, and gallium germanate UCSB-3GaGe. The structure has a 3D 8-ring channel system with protonated ethylenediammonium cations in the channel junctions. The material turns amorphous upon removal of the organic template on heating.

Introduction

The open framework structures of zeolitic aluminosilicates such as those for zeolite A, X, and Y, early on became important for industrial applications. During the last 50 years, extensive efforts have continuously been made to synthesize new types of zeolite materials, partly with hitherto unknown topologies, that possibly may lead to new applications. In the early 1980s the chemical compositional domain of zeolite-type materials was broadened to include aluminophosphates.¹ More recently, the chemical domain was further expanded to a variety of elements that are capable of forming tetrahedrally linked open framework compounds. The incorporation of divalent elements such as Be^{2+} , Zn^{2+} , Mg^{2+} , Ni^{2+} , Mn^{2+} , and Co^{2+} into aluminophosphates gave rise to the so-called metalloaluminophosphates (MAPOs), which represent important compounds, owing to their potential catalytic and adsorptive properties. Until recently the highest degree of substitution for Al^{3+} by a divalent element was 38% in $\text{CoAlPO}_4\text{-50}$;² however, Stucky and co-workers have now been able to increase the solid solution substitution limit to about 90%.^{3,4} On the other hand there exist zeolitic phosphates with just divalent Be^{2+} ,^{5–11} Zn^{2+} ,^{7,12–15} or Co^{2+} .^{16,17}

Another divalent element which plays a major role in MAPO synthesis is magnesium. Several unique structures such as DAF-1,¹⁸ STA-1,¹⁹ and STA-2²⁰ have only been synthesized as MgAlPO_4 . UiO-16²¹ was the first example of an organically templated layered magnesium phosphate, and the present paper reports on the synthesis and crystal structure of the first example of an organically templated open framework magnesium phosphate, here denoted UiO-20. The compound has a zeolite-type magnesium phosphate framework with alternating linkage of corner-shared MgO_4 and PO_4 tetrahedra. The compound has the DFT topology and is isostructural with compounds such as the cobalt phosphate DAF-2¹⁶ and the zinc phosphate DAF-3.¹³

* Correspondence should be sent to Professor Helmer Fjellvåg: Department of Chemistry, University of Oslo, P.O. Box 1033 Blindern, N-0315 Oslo, Norway. E-mail: helmer.fjellvag@kjemi.uio.no. Telephone: +4722855564. Fax: +4722855565.

(1) Wilson, S. T.; Lok, B. M.; Messina, C. A.; Cannan, T. R.; Flanigan, E. M. *J. Am. Chem. Soc.* **1982**, *104*, 1146.

(2) Bennes, I. M.; Marcus, B. K. *Innovation of Zeolite Materials Science*; Elsevier Science Publishers: Amsterdam, 1988; p 269.

(3) Feng, P.; Bu, X.; Stucky, G. D. *Nature* **1997**, *388*, 735.

(4) Bu, X.; Feng, P.; Stucky, G. D. *Science* **1997**, *278*, 2080.

(5) Havey, G.; Meier, W. M. *Stud. Surf. Sci. Catal.* **1989**, *49*, 411.

(6) Havey, G.; Baerlocher, C. Z. *Kristallogr.* **1992**, *201*, 113.

(7) Gier, T. E.; Stucky, G. D. *Nature* **1991**, *349*, 508.

(8) Harrison, W. T. A.; Gier, T. E.; Moran, K. L.; Nicol, J. M.; Eckert, H.; Stucky, G. D. *Chem. Mater.* **1991**, *3*, 27.

(9) Gier, T. E.; Harrison, W. T. A.; Stucky, G. D. *Angew. Chem.* **1991**, *103*, 1191.

(10) Harrison, W. T. A.; Gier, T. E.; Stucky, G. D. *Zeolites* **1993**, *13*, 242.

(11) Bu, X.; Gier, T. E.; Stucky, G. D. *Microporous Mesoporous Mater.* **1998**, *26*, 61.

(12) Yakubovich, O. V.; Karimova, O. V.; Mel'nikov, O. K. *Cryst. Rep.* **1994**, *39*, 564.

(13) Jones, R. H.; Chen, J.; Sankar, G.; Thomas, J. M. *Zeolites and Microporous Materials: State of the Art 1994*; Elsevier: New York, 1994; p 2229.

(14) Harrison, W. T. A.; Gier, T. E.; Stucky, G. D.; Broach, R. W.; Bedard, R. A. *Chem. Mater.* **1996**, *8*, 145.

(15) Broach, R. W.; Bedard, R. L.; Song, S. G.; Pluth, J. J.; Bram, A.; Riekel, C.; Weber, H. P. *Chem. Mater.* **1999**, *11*, 2076.

(16) Chen, J.; Jones, R. H.; Natarajan, S.; Hursthouse, M. B.; Thomas, J. M. *Angew. Chem., Int. Ed. Engl.* **1994**, *33*, 639.

(17) Feng, P.; Bu, X.; Tolbert, S. H.; Stucky, G. D. *J. Am. Chem. Soc.* **1997**, *119*, 2497.

(18) Wright, P. A.; Jones, R. H.; Natarajan, S.; Bell, R. G.; Chen, J.; Hursthouse, M. B.; Thomas, J. M. *J. Chem. Soc., Chem. Commun.* **1993**, 633.

(19) Noble, G. W.; Wright, P. A.; Lightfoot, P.; Morris, R. E.; Hudson, K. J.; Kvik, A.; Graafsma, H. *Angew. Chem., Int. Ed. Engl.* **1997**, *36*, 81.

(20) Noble, G. W.; Wright, P. A.; Kvik, A. *J. Chem. Soc., Dalton Trans.* **1997**, 4485.

(21) Kongshaug, K. O.; Fjellvåg, H.; Lillerud, K. P. *Chem. Mater.* **1999**, *11*, 2872.

Table 1. Crystal Data and Structure Refinement for UiO-20

empirical formula	Mg ₄ P ₄ O ₁₆ N ₄ C ₄ H ₂₀
formula weight	601.36
temperature	150(2) K
wavelength	0.71073 Å
crystal system	monoclinic
space group	<i>C2/c</i>
unit cell dimensions	<i>a</i> = 20.9098(8) Å <i>b</i> = 17.8855(7) Å <i>c</i> = 14.7913(6) Å β = 134.842(2)°
volume	3922.3(3) Å ³
<i>Z</i>	8
density (calculated)	2.037 g cm ⁻³
absorption coefficient	0.603 mm ⁻¹
<i>F</i> (000)	2464
crystal size	0.12 × 0.11 × 0.08 mm
θ range for data collection	1.78–23.43°
index ranges	−23 ≤ <i>h</i> ≤ 23; −19 ≤ <i>k</i> ≤ 19; −16 ≤ <i>l</i> ≤ 16
reflections collected	13912
independent reflections	2826 [<i>R</i> (int) = 0.1153]
reflections observed (>2 σ)	1922
refinement method	full-matrix least-squares on <i>F</i> ²
data/restraints/parameters	2826/0/298
goodness-of-fit on <i>F</i> ²	1.401
final <i>R</i> indices [<i>I</i> > 2 σ (<i>I</i>)]	<i>R</i> ₁ = 0.0621; <i>wR</i> ₂ = 0.0919
<i>R</i> indices (all data)	<i>R</i> ₁ = 0.1007; <i>wR</i> ₂ = 0.0994
largest diff. peak and hole	0.400 and −0.562 e Å ⁻³

Experimental Section

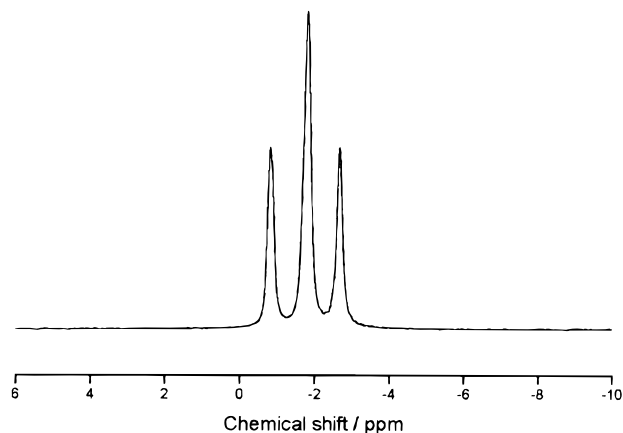
UiO-20 was prepared hydrothermally by first mixing Mg₃(PO₄)₂·8H₂O (5.45 g, Fluka), 85 wt % H₃PO₄ (3.10 g, Merck), and deionized water (9.03 g) followed by stirring at room temperature for 15 min. Thereafter ethylenediamine (2.42 g, Fluka) was added, and the mixture was stirred for another 10 min. The molar composition of the mother solution was 3 MgO:2P₂O₅:3ethylenediamine:50H₂O. This solution was transferred to a Teflon-lined steel autoclave, which was filled to 80% of maximum volume, and heated at 150 °C for 24 h. The initial and final pH was 8.8 and 8.1, respectively. The product was recovered by filtration and washed by deionized water. The yield based on magnesium was 40%.

Characterization of the product was initially performed by powder X-ray diffraction (PXD) using a Siemens D5000 diffractometer in Bragg–Brentano geometry. The diffractometer was equipped with an incident beam monochromator giving Cu K α ₁ (λ = 1.540598 Å) radiation and a Braun positional sensitive detector. The obtained diffraction pattern did not correspond to any known magnesium phosphate compound. High-resolution PXD data were subsequently collected in transmission geometry with the sample in a rotating 0.5-mm borosilicate capillary. Data were collected for the 2θ range 10–90° (counting time 12 s).

Thermogravimetric analysis (TGA) was performed on a Scientific Rheometric STA 1500 instrument. The sample was heated from room temperature to 700 °C at a rate of 5 K min⁻¹ in a flow of oxygen. This heat treatment gave a black, X-ray amorphous residue, probably carbon, that was taken as indicative of incorporation of organic species in the obtained, new compound. Powder X-ray diffraction showed the residue to be amorphous.

Solid state ³¹P MAS NMR data were recorded with a Bruker DMX-200 spectrometer. The spinning rate was 8.0 kHz, and the spectrum was collected during 16 scans using 100 s repetition time.

A suitable single crystal was selected and mounted on a Siemens SMART-CCD diffractometer. Intensity data covering a hemisphere of reciprocal space were collected at 150 K by means of 1525 frames ($\Delta\theta$ = 0.3°; 30 s per frame). Integration and data reduction were done using the SAINT software.²² An

**Figure 1.** ³¹P MAS NMR spectrum of UiO-20.**Table 2. Atomic Coordinates and Equivalent Isotropic Displacement Parameters (Å² × 10³) for UiO-20^a**

atom	<i>x</i>	<i>y</i>	<i>z</i>	<i>U</i> (eq)
Mg(1)	0.6337(2)	0.5791(1)	0.8697(2)	9(1)
Mg(2)	0.1339(1)	0.5828(1)	0.8798(2)	9(1)
Mg(3)	0.5134(1)	0.6686(1)	0.3938(2)	8(1)
Mg(4)	0.0011(1)	0.6701(1)	0.3846(2)	10(1)
P(1)	0.4880(1)	0.6450(1)	0.5859(2)	9(1)
P(2)	0.8503(1)	0.6002(1)	0.1141(2)	8(1)
P(3)	0.6496(1)	0.3955(1)	0.8964(2)	9(1)
P(4)	−0.0044(1)	0.6504(1)	0.5961(2)	8(1)
O(1)	0.5787(3)	0.5965(3)	0.9299(5)	20(1)
O(2)	0.0369(3)	0.7735(3)	0.4253(4)	15(1)
O(3)	0.5851(3)	0.6279(2)	0.7143(4)	17(1)
O(4)	0.4803(3)	0.6232(2)	0.4771(4)	11(1)
O(5)	0.9112(3)	0.6126(3)	0.0934(4)	19(1)
O(6)	0.8792(3)	0.6510(2)	0.2222(4)	14(1)
O(7)	0.8516(3)	0.5192(2)	0.1478(4)	11(1)
O(8)	0.7528(3)	0.6233(2)	−0.0102(4)	14(1)
O(9)	0.6387(3)	0.4745(3)	0.8498(4)	15(1)
O(10)	0.5918(3)	0.3403(2)	0.7850(4)	13(1)
O(11)	0.7491(3)	0.3707(2)	0.9848(4)	11(1)
O(12)	0.6227(3)	0.3894(3)	0.9709(4)	15(1)
O(13)	0.0852(3)	0.6474(2)	0.7371(4)	16(1)
O(14)	−0.0463(3)	0.7283(2)	0.5554(4)	11(1)
O(15)	0.9297(3)	0.5921(2)	0.5710(5)	16(1)
O(16)	0.0140(3)	0.6254(2)	0.5161(4)	10(1)
N(1)	0.1204(4)	0.5010(3)	0.6262(5)	13(1)
N(2)	0.6261(4)	0.5053(3)	0.6242(5)	14(1)
N(3)	0.7586(4)	0.2534(3)	0.1335(5)	13(1)
N(4)	0.7341(4)	0.7513(3)	0.1062(5)	15(1)
C(1)	0.7169(4)	0.4716(4)	0.7168(6)	14(2)
C(2)	0.2119(4)	0.5328(4)	0.7085(6)	14(2)
C(3)	0.7604(4)	0.2203(4)	0.2269(6)	11(2)
C(4)	0.7403(4)	0.7825(4)	0.2040(6)	13(2)

^a *U*(eq) is defined as one-third of the trace of the orthogonalized *U*_{*ij*} tensor. Calculated standard deviations in parentheses.

absorption correction based on symmetry equivalent reflections was applied using SADABS.²³ Further crystal and experimental data are given in Table 1.

The crystal structure was determined and refined using the SHELXTL program package.²⁴ A structure solution was first achieved in the small tetragonal unit cell, *a* = 10.4702 Å and *c* = 8.941 in space group *P*₄₂/*n*. However, the ³¹P MAS NMR data indicated the existence of a supercell. The ³¹P NMR spectrum shows three peaks in the intensity ratio 1:2:1, see Figure 1. This indicates that there are four crystallographically distinct P positions. The subcell described above has only one nonequivalent P position. Therefore, a 4-fold centered monoclinic supercell was adopted: *a* = 20.9098 Å, *b* = 17.8855 Å, *c*

(23) Sheldrick, G. M. *SADABS, Empirical Absorption Corrections Program*; University of Göttingen: Göttingen, 1997.

(24) Sheldrick, G. M. *SHELXTL Version 5.0*; BrukerAnalytical X-ray Instruments Inc.: Madison, WI, 1994.

(22) SAINT Integration Software, Version 4.05; BrukerAnalytical X-ray Instruments Inc.: Madison, WI, 1995.

Table 3. Selected Interatomic Distances [Å] and Bond Angles [deg] for UiO-20^a

Mg(1)–O(9)	1.907(5)	O(9)–Mg(1)–O(1)	110.4(2)
Mg(1)–O(1)	1.914(5)	O(9)–Mg(1)–O(8)	111.6(2)
Mg(1)–O(8)	1.935(5)	O(1)–Mg(1)–O(8)	108.2(2)
Mg(1)–O(3)	1.946(5)	O(9)–Mg(1)–O(3)	107.4(2)
		O(1)–Mg(1)–O(3)	119.5(2)
		O(8)–Mg(1)–O(3)	99.4(2)
Mg(2)–O(15)	1.921(5)	O(15)–Mg(2)–O(7)	114.5(2)
Mg(2)–O(7)	1.940(5)	O(15)–Mg(2)–O(11)	106.1(2)
Mg(2)–O(11)	1.944(5)	O(7)–Mg(2)–O(11)	110.5(2)
Mg(2)–O(13)	1.949(5)	O(15)–Mg(2)–O(13)	112.7(2)
		O(7)–Mg(2)–O(13)	111.7(2)
		O(11)–Mg(2)–O(13)	100.3(2)
Mg(3)–O(10)	1.911(4)	O(10)–Mg(3)–O(14)	111.4(2)
Mg(3)–O(14)	1.927(5)	O(10)–Mg(3)–O(4)	105.3(2)
Mg(3)–O(4)	1.962(4)	O(14)–Mg(3)–O(4)	109.8(2)
Mg(3)–O(12)	1.981(5)	O(10)–Mg(3)–O(12)	119.2(2)
		O(14)–Mg(3)–O(12)	109.1(2)
		O(4)–Mg(3)–O(12)	101.3(2)
Mg(4)–O(5)	1.922(5)	O(5)–Mg(4)–O(2)	110.2(2)
Mg(4)–O(2)	1.925(5)	O(5)–Mg(4)–O(6)	112.3(2)
Mg(4)–O(6)	1.936(5)	O(2)–Mg(4)–O(6)	116.1(2)
Mg(4)–O(16)	1.937(4)	O(5)–Mg(4)–O(16)	99.7(2)
		O(2)–Mg(4)–O(16)	109.6(2)
		O(6)–Mg(4)–O(16)	107.6(2)
P(1)–O(1)	1.513(5)	O(1)–P(1)–O(2)	108.9(3)
P(1)–O(2)	1.518(5)	O(1)–P(1)–O(3)	110.2(3)
P(1)–O(3)	1.544(5)	O(2)–P(1)–O(3)	112.1(3)
P(1)–O(4)	1.549(4)	O(1)–P(1)–O(4)	106.7(3)
		O(2)–P(1)–O(4)	110.6(3)
		O(3)–P(1)–O(4)	108.2(3)
P(2)–O(5)	1.521(4)	O(5)–P(2)–O(7)	112.4(3)
P(2)–O(7)	1.525(5)	O(5)–P(2)–O(6)	110.5(3)
P(2)–O(6)	1.545(4)	O(7)–P(2)–O(6)	108.4(3)
P(2)–O(8)	1.556(5)	O(5)–P(2)–O(8)	108.0(3)
		O(7)–P(2)–O(8)	110.2(2)
		O(6)–P(2)–O(8)	107.2(3)
P(3)–O(9)	1.518(5)	O(9)–P(3)–O(10)	111.1(3)
P(3)–O(10)	1.531(4)	O(9)–P(3)–O(11)	109.4(3)
P(3)–O(11)	1.548(5)	O(10)–P(3)–O(11)	107.2(2)
P(3)–O(12)	1.555(5)	O(9)–P(3)–O(12)	112.0(3)
		O(10)–P(3)–O(12)	108.1(2)
		O(11)–P(3)–O(12)	108.9(2)
P(4)–O(14)	1.524(5)	O(14)–P(4)–O(13)	112.3(3)
P(4)–O(13)	1.534(5)	O(14)–P(4)–O(16)	110.2(2)
P(4)–O(16)	1.546(4)	O(13)–P(4)–O(16)	107.8(3)
P(4)–O(15)	1.550(5)	O(14)–P(4)–O(15)	110.7(3)
		O(13)–P(4)–O(15)	109.2(3)
		O(16)–P(4)–O(15)	106.3(2)
N(1)–C(2)	1.476(8)	N(2)–C(1)–C(2)	109.9(5)
N(2)–C(1)	1.474(8)	N(1)–C(2)–C(1)	110.9(5)
N(3)–C(3)	1.480(8)	N(3)–C(3)–C(4)	109.3(5)
N(4)–C(4)	1.469(8)	N(4)–C(4)–C(3)	110.4(5)
C(1)–C(2)	1.522(9)		
C(2)–C(1)	1.522(9)		
C(3)–C(4)	1.519(8)		
C(4)–C(3)	1.519(8)		

^a Calculated standard deviations in parentheses.

= 14.7913 Å, and $\gamma = 134.842^\circ$ in space group $C2/c$. The direct method solution gave the Mg and P positions, whereas O, C, and N atoms were located by difference Fourier analyses. No hydrogen position could be located from the maps; however, hydrogen atoms were placed geometrically and refined in the riding mode. The last cycles of the refinements included atomic coordinates for all atoms, anisotropic displacement parameters for all non-hydrogen atoms and isotropic displacement parameters for all hydrogen atoms. The final atomic coordinates are given in Table 2, whereas selected bond distances and angles are listed in Table 3. Figure 2 shows the close correspondence between the experimentally obtained powder X-ray diffraction pattern of the bulk sample isolated from the autoclave and

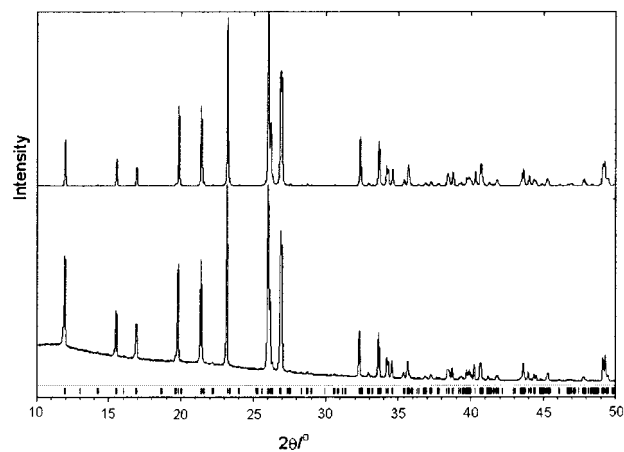


Figure 2. Simulated (top) and experimental (bottom) powder X-ray diffractogram for UiO-20 (Cu K α_1 radiation, $\lambda = 1.540598$ Å).

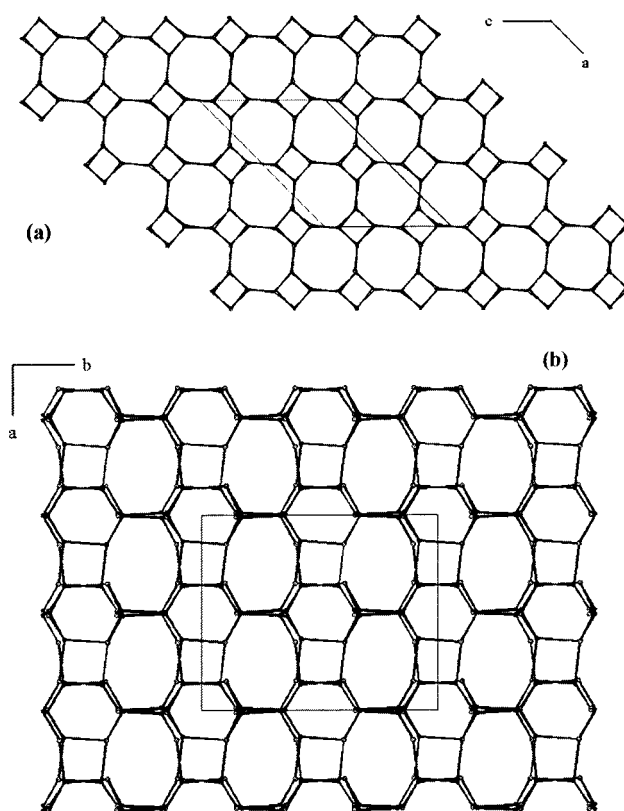


Figure 3. Crystal structure of UiO-20 seen along (a) [010] and (b) [001] showing eight-membered rings. For clarity, template molecules occluded in the framework and framework oxygens are omitted. The unit cell is indicated by thin lines.

that simulated on the basis of the single-crystal structure solution.

Results and Discussion

The asymmetric unit of UiO-20 contains $[\text{NH}_3(\text{CH}_2)_2\text{-NH}_3]_2^{4+}[\text{Mg}_4(\text{PO}_4)_4]^{4-}$. The framework consists strictly of alternating MgO_4 and PO_4 tetrahedra. The structure is characterized by a 3D eight-membered ring channel system with channels parallel to the crystallographic axes. The channel along [010] has dimensions 6.4×6.5 Å, Figure 3a. The channels along [100] and [001] have similar characteristics and dimensions 7.4×4.5 Å, Figure 3b. The diprotonated ethylenediammonium cat-

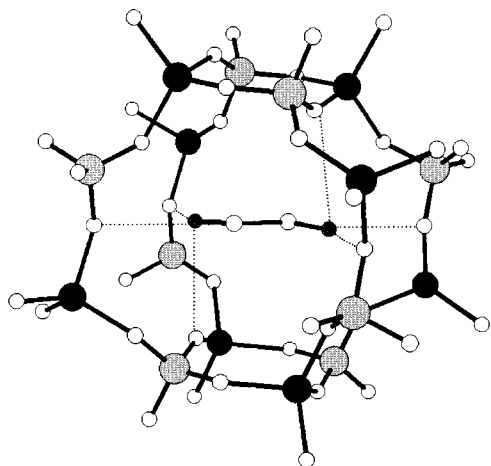


Figure 4. Positioning of ethylenediammonium ions accommodated in the channel junctions. Dotted lines indicate hydrogen-bonding interactions. Mg atoms are indicated with filled circles; P atoms, with shaded circles.

Table 4. Hydrogen Bonding Interactions in UiO-20

interaction	distance (Å)
N(1)⋯O(7)	2.98
N(1)⋯O(15)	2.84
N(1)⋯O(16)	2.73
N(2)⋯O(3)	2.99
N(2)⋯O(4)	2.79
N(2)⋯O(12)	2.91
N(3)⋯O(11)	2.76
N(3)⋯O(12)	3.19
N(3)⋯O(13)	2.94
N(4)⋯O(2)	2.97
N(4)⋯O(6)	2.83
N(4)⋯O(8)	2.77

Table 5. Bond Valence Analysis for UiO-20

	P(1)	P(2)	P(3)	P(4)	Mg(1)	Mg(2)	Mg(3)	Mg(4)	Σ
O(1)	1.32				0.55				1.87
O(2) ^a	1.31						0.53		1.84
O(3) ^a	1.22				0.50				1.72
O(4) ^a	1.20						0.48		1.68
O(5)		1.30						0.54	1.84
O(6) ^a		1.21						0.52	1.73
O(7) ^a		1.28				0.51			1.79
O(8) ^a		1.18			0.52				1.70
O(9)			1.31		0.56				1.87
O(10)			1.26				0.55		1.81
O(11) ^a			1.21			0.51			1.72
O(12) ^a			1.18				0.46		1.64
O(13) ^a				1.25		0.50			1.75
O(14)				1.29			0.53		1.82
O(15) ^a				1.20		0.54			1.74
O(16) ^a				1.21				0.52	1.73
Σ	5.05	4.97	4.96	4.95	2.13	2.06	2.02	2.11	

^a Involved in additional hydrogen bonding interactions, see Table 4.

ions are accommodated in the channel junctions and are hydrogen bonded to oxygen atoms of the framework, see Table 4 and Figure 4.

A bond valence analysis²⁵ for UiO-20 shows that the calculated valences are close to the expected values of 2 and 5 for magnesium and phosphorus, respectively (Table 5). Some of the valences calculated for the oxygen atoms are rather low; however, their valences are partly fulfilled by means of hydrogen-bonding interactions with ethylenediammonium cations.

(25) Brown, I. D.; Altermatt, D. *Acta Crystallogr.* **1985**, B41, 244.



Figure 5. Bifurcated hexagonal-square (bhs) chain running along [010].

One interesting aspect of UiO-20 is the presence of tetrahedrally coordinated magnesium. Magnesium has a strong preference for octahedral coordination, and other examples of structures with tetrahedrally coordinated magnesium are rather scarce. In phosphate-based compounds, MgAPOs, Mg is known to substitute partly for tetrahedral Al in the framework.^{26,27} Other examples include the diphosphate $\text{Mg}_2\text{P}_2\text{O}_7 \cdot \text{H}_2\text{O}$ ²⁸ and the α , β , and γ forms of KMgPO_4 .²⁹ Also in spinels such as MgAl_2O_4 ³⁰ and MgTi_2O_4 ³¹ there are tetrahedrally coordinated magnesium. In UiO-20 there is no terminal or bridging water molecules or hydroxyl groups leading to higher than tetrahedral coordination for magnesium.

The four-connected 3D net in UiO-20 can be decomposed and described by means of two subunits, either in terms of a 2D net or as a 1D chain. The 2D 4.8^2 net,³² see Figure 3a, forms when stacked along [010] the four-connected 3D net of UiO-20. The 4.8^2 net is a common structural motif seen in many zeolite topologies including ABW, GIS, MER, PHI, and ACO. The 1D chain in the alternative description is a bifurcated hexagonal-square chain (bhs), see Figure 5 running along [010]. When cross-linked they convert into the four-connected 3D net of UiO-20.

(26) Han, S. X.; Smith, J. V.; Pluth, J. J.; Richardson, J. W. *Eur. J. Mineral.* **1990**, 2, 787.

(27) Smith, J. V.; Pluth, J. J.; Andries, K. J. *Zeolites* **1993**, 13, 166.

(28) Kongshaug, K. O.; Fjellvåg, H.; Lillerud, K. P. *Solid State Sci.*, in press.

(29) Wallez, G.; Colbeau-Justin, C.; Le Mercier, T.; Quarton, M.; Robert, F. *J. Solid State Chem.* **1998**, 136, 175.

(30) Bacon, G. E. *Acta Crystallogr.* **1952**, 5, 684.

(31) Leclercq, A. Thesis, Bordeaux University, 1962.

(32) Smith, J. V. *Chem. Rev.* **1988**, 88, 149.

The framework topology of UiO-20 is identical to the theoretical net 39 proposed early in the 1960s,³³ now assigned the three-letter code DFT by IZA. A number of compounds with different compositions are isostructural with UiO-20; e.g., the cobalt phosphate DAF-2,¹⁶ the zinc phosphate DAF-3,¹³ the zinc arsenate UCSB-3ZnAs,³⁴ the gallium germanate UCSB-3GaGe,³⁵ and the aluminum cobalt phosphate ACP-3.³⁴

The different compounds with the DFT topology have in common that they all have been synthesized with ethylenediamine as organic template. Ethylenediamine has recently also been used in the cobalt, aluminum, and phosphate system to synthesize the zeolite topologies MER,³ GIS,³⁶ and ACO.³ Both MER and GIS are naturally occurring aluminosilicate minerals and can also be synthesized in this system. The DFT and ACO topologies have on the other hand not been synthesized as aluminosilicates. The ACO topology has just been synthesized as a aluminum cobalt phosphate, but O'Keeffe et al.³⁷ have pointed out that there is no geometrical reason it has not yet been found as a silicate or germanate. DFT has already been found as a germanate, but it may be difficult to synthesize it as a silicate as the bhs chain is rarely observed in silicate compounds. The few examples include the nonzeolitic isostructural aluminosilicates banalsite, BaNa₂Al₄Si₄O₁₆,³⁸ and lisetite, CaNa₂Al₄Si₄O₁₆,³⁹ and titanosilicate narsarsukite, Na₂TiOSi₄O₈.⁴⁰

The chemical shift values of -0.82 , -1.80 , and -2.67 ppm for the resonances in the ³¹P MAS NMR spectrum

(Figure 1) fall inside the appropriate range (-30 to 12 ppm) reported for a large number of orthophosphates,⁴¹ and is also close to values reported for P(4Mg) environments in magnesium-substituted aluminophosphates.⁴² Müller et al.⁴³ have suggested an empirical correlation between ³¹P chemical shift and average P–O–Al bond angle in aluminophosphates where the chemical shift decreases with increasing average bond angle. The relevant average bond angles in UiO-20 are: $\angle(\text{P}(1)\text{--O--Mg}) = 140.7^\circ$, $\angle(\text{P}(2)\text{--O--Mg}) = 139.7^\circ$, $\angle(\text{P}(3)\text{--O--Mg}) = 136.5^\circ$, and $\angle(\text{P}(4)\text{--O--Mg}) = 136.3^\circ$. These values combined with an observed 1:2:1 intensity ratio in the spectrum makes it impossible to assign the different resonances to the different crystallographic P sites in UiO-20 using the average angle correlation. From the bond angles alone one would expect a 2:1:1 ratio. The reason for the failure is possibly related to the presence of organic template in the channels. The ethylenediamine modifies the secondary coordination sphere of the phosphorus atoms and interacts with the framework oxygen atoms of the primary PO₄-tetrahedra via hydrogen bonds. This effect is different among the nonequivalent P atoms and has a certain influence on the NMR signals. Similar effects have been reported in the literature.⁴⁴

Supporting Information Available: Tables of bond lengths and angles, anisotropic displacement parameters, hydrogen coordinates and isotropic displacement parameters, and structure factors for UiO-20. This material is available free of charge via the Internet at <http://pubs.acs.org>.

CM991175E

- (33) Smith, J. V.; Rinaldi, F. *Mineral. Mag.* **1962**, *33*, 202.
(34) Bu, X.; Feng, P.; Gier, T. E.; Stucky, G. D. *J. Solid State Chem.* **1998**, *136*, 210.
(35) Bu, X.; Feng, P.; Gier, T. E.; Zhao, D.; Stucky, G. D. *J. Am. Chem. Soc.* **1998**, *120*, 13389.
(36) Gainsford, G. J.; Morgan, K. R.; Rae, A. D. *Acta Crystallogr.* **1998**, *C54*, 1564.
(37) O'Keeffe, M.; Yaghi, O. M. *Chem. Eur. J.* **1999**, *5*, 2796.
(38) Haga, N. *Mineral. J.* **1973**, *7*, 262.
(39) Rossi, G.; Oberti, R.; Smith, D. C. *Am. Mineral.* **1986**, *71*, 1378.
(40) Peacor, D. R.; B rger, M. J. *Am. Mineral.* **1962**, *47*, 539.

- (41) Hartmann, P.; Vogel, J.; Schnabel, B. *J. Magn. Reson.* **1994**, *111*, 110.
(42) Akolelar, D. B.; Howe, R. F. *J. Chem. Soc., Faraday Trans.* **1997**, *93*, 3263.
(43) M ller, D.; Jahn, E.; Ladwig, G.; Haubenreisser, U. *Chem. Phys. Lett.* **1984**, *109*, 332.
(44) Caldarelli, S.; Meden, A.; Tuel, A. *J. Phys. Chem. B* **1999**, *103*, 5477.